This document is the Submitted Manuscript version of a Published Work that appeared in final form in *Science Of The Total Environment*, March 2017.

Online version:
https://www.sciencedirect.com/science/article/abs/pii/S0048969716328509

DOI: https://doi.org/10.1016/j.scitotenv.2016.12.161

Solar radiation as a swift pathway for PAH photodegradation: A field study

Montse Marquès [a,b], Montse Mari [a,b], Jordi Sierra [b,c], Martí Nadal [a,*], José L. Domingo [a]

[a] *Laboratory of Toxicology and Environmental Health, School of Medicine, IISPV, Universitat Rovira i Virgili, Sant Llorenç 21, 43201 Reus, Catalonia, Spain*

[b] *Environmental Engineering Laboratory, Departament d'Enginyeria Quimica, Universitat Rovira i Virgili, Av. Països Catalans 26, 43007 Tarragona, Catalonia, Spain*

[c] *Laboratory of Soil Science, Faculty of Pharmacy, Universitat de Barcelona, Av. Joan XXIII s/n, 08028 Barcelona, Catalonia, Spain*

---

* Corresponding author. Tel.: +34 977 758930; fax: +34 977 759322.

E-mail address: marti.nadal@urv.cat (M. Nadal).

ABSTRACT

The photodegradation of polycyclic aromatic hydrocarbons (PAHs) may be an important degradation pathway of PAHs in regions with a high solar radiation. The present investigation was aimed at studying the photodegradation of PAHs after their deposition on surface soils with different textures. Photodegradation by-products were also identified and semi-quantified, as well as correlated with the decrease of parent compounds. The experiment was performed by deploying soil samples spiked with a mixture of the 16 US EPA priority PAHs in a methacrylate box, exposed to solar radiation for 7 days. As hypothesized, the individual PAHs were volatilized, sorbed and/or photodegraded, depending on their physicochemical properties, as well as the soil characteristics. Low and medium molecular weight PAHs were more sorbed and photodegraded in fine-textured Regosol soil, while a higher volatilization was observed in the coarse-textured Arenosol soil. In contrast, high molecular weight PAHs were more photodegraded in Arenosol soil. Specially low half-lives were noted for anthracene and benzo(*a*)pyrene, agreeing with previous findings at laboratory scale. However, photodegradation rates were up to 20-times higher under solar radiation than those observed in soils subject to radiation in a climate chamber. Nine by-products were identified, including oxy-, nitro- and hydroxy-PAHs, whose toxic and mutagenic potential might be higher than the 16 priority PAHs.

Keywords:

Polycyclic aromatic hydrocarbons (PAHs)

Soil

Solar radiation

Photodegradation

By-products

1. Introduction

Polycyclic aromatic hydrocarbons (PAHs) form a group of over 200 different organic compounds with two or more fused aromatic rings (Domingo and Nadal, 2015). Since some PAHs have been classified as carcinogenic and teratogenic, this family of pollutants has reached a considerable international concern (Chen et al., 2016). PAHs may enter the environment from both natural (e.g. plant synthesis, organic matter diagenesis, and forest fires) and anthropogenic (e.g., industrial activities, residential heating, power generation, incineration, and traffic) sources (Nadal et al., 2009). Once released to the atmosphere, gas phase PAHs are able to travel long distances before their deposition. Because of their low solubility and hydrophobic nature, high molecular weight (HMW) PAHs tend to be sorbed to particulates, being also widely transported through atmospheric routes. Consequently, they may mean a hazard, not only to human populations living in urban areas, but also to natural ecosystems (Augusto et al., 2015; Hu et al., 2014; Hung et al., 2005; Nadal et al., 2011; Ohkouchi et al., 1999).

As organic molecules, PAHs may undergo various natural processes such as biodegradation, chemical transformation, and photolysis reactions (Jia et al., 2015). It has been suggested that the photolysis of PAHs on soil surfaces plays an important role in the environmental fate of these chemicals (EL-Saeid et al., 2015). Upon light irradiation, PAHs can absorb light energy to reach photo-excited states. Therefore, they react with molecular oxygen and coexisting chemicals to produce reactive oxygen species (ROS) and other reactive intermediates, such as oxygenated PAHs and free radicals (Fu et al., 2012).

In recent years, the photodegradation of organic compounds in various environmental matrices has been largely studied, mostly for remediation purposes. One of the applications is the use of light lamps to remove antibiotics in water (Batchu et al., 2014; Ge et al., 2010; Pereira et al., 2007). Regarding PAHs, most photodegradation investigations have been performed at laboratory scale by means of artificial light (Gupta and Gupta, 2015; Marquès et al., 2016a,b; Zhang et al., 2006, 2008, 2010). Natural sunlight, whose intensity is notably higher than that emitted by laboratory lamps, has been used to study the photodegradation in air of different organic compounds such as organophosphate pesticides (Borrás et al., 2015), aromatic compounds (Pereira et al., 2015), organochlorines (Vera et al., 2015), and herbicides (Muñoz et al., 2014). However,

there is a gap in the knowledge of the natural photodegradation of PAHs in soils and other environmental matrices.

It has been hypothesized that PAH photodegradation would be higher and faster under solar radiation than under lab-controlled light lamps. Consequently, PAH by-products, which may be even more toxic than their parent compounds, can be more easily generated (Ras et al., 2009). The evaluation of PAHs degradation products is highly valuable to assess human health risks derived from exposure to such compounds, which are not considered so far by environmental regulations.

This study was aimed at assessing the photodegradation of the 16 US EPA priority PAHs under solar radiation in two types of soils frequently found in the Mediterranean region, as it naturally occurs. In addition, PAHs photodegradation by-products were identified and semi-quantified. The current results were finally compared to those obtained in a previous study performed at laboratory scale (Marquès et al., 2016a,b).

2. Materials and methods

2.1. Experiment design: photodegradation of PAHs

Details of soil characteristics, as well as contamination procedure, were recently reported (Marquès et al., 2016b). Briefly, two different soils were collected from the A horizon of remotes areas of Catalonia (NE of Spain): a) an acidic and coarse-textured Arenosol soil, with granitic origin, and b) a fine-textured Regosol soil, formed by sedimentary materials. Ten grams of air-dried soil were weighed and deployed in uncovered glass Petri dishes of 7 cm of diameter. A solution containing the 16 US EPA priority PAHs at 2000 µg mL^{-1} in dichloromethane:benzene (naphthalene 99.3% purity, acenaphthylene 99.2% purity, acenaphthene 99.3% purity, fluorene 98.2% purity, phenanthrene 97.6% purity, anthracene 99.0% purity, fluoranthene 99.5% purity, pyrene 98.9% purity, benzo(*a*)anthracene 98.5% purity, chrysene 97.4% purity, benzo(*b*)fluoranthene 97.3% purity, benzo(*k*)fluoranthene 99.5% purity, benzo(*a*)pyrene 95.0% purity, dibenzo(*a,h*)anthracene 99.0% purity, benzo(*ghi*)perylene 99.4% purity, and indeno (*123-c,d*)pyrene 99.7% purity) was purchased at Supelco® (Bellefonte, PA, USA). Each soil sample was 10-times spiked with 25 µL of such solution diluted down to 100 µg mL^{-1} in hexane/dichloromethane (1:1) (Scharlau Chemie S. A., Barcelona, Spain), driving to a Σ16 PAHs concentration of 40 µg g^{-1} of soil.

126 The present study was carried out in a UV-light permeable methacrylate box placed
127 on the roof of the School of Chemical Engineering, Universitat Rovira i Virgili, Tarragona
128 (Catalonia, Spain). Although the methacrylate box protected the samples from the wind,
129 it allowed the penetration of the whole light spectrum coming from solar radiation. The
130 box owned eight holes of 2 cm of diameter, which facilitated the exchange of air and
131 softened any temperature increase. The temperature inside the box was registered by
132 using the temperature data logger EBI 300 (Ebro®, Ingolstadt, Germany) with 30 minutes
133 of time-span. Once the samples were contaminated with PAHs, they were deployed inside
134 the methacrylate box and exposed to sunlight. In addition to irradiated samples, dark
135 controls were covered with aluminum foil. The experiment was conducted during late
136 boreal winter, from 8 to 15 March 2016. Triplicates of irradiated samples and dark
137 controls of each soil were removed from the methacrylate box after the following
138 exposure times: 0.5, 1, 2, 3, 6, 24, 48, 72, 96 and 168 hours. Simultaneously,
139 environmental parameters such as precipitation, humidity and global solar irradiance
140 were continuously monitored in a meteorological station located nearby (Constantí,
141 Tarragona, Spain).
142
143 *2.2. PAH extraction and analysis*
144
145 The methodology for the extraction and analysis of PAHs in soils was previously
146 reported (Marquès et al., 2016a). Briefly, 30 mL of hexane/dichloromethane (1:1)
147 (Scharlau Chemie S. A., Barcelona, Spain) were added to soil samples. Then, each sample
148 was 3-times subjected to an ultrasonic bath programmed for 10 min. After each step, the
149 solvent was filtered. Subsequently, the extract was slowly concentrated with a rotatory
150 evaporator down to 2 mL, and finally with a gentle stream of purified N_2 (99.9999%). In
151 addition to irradiated and dark control samples, 10 g of soil free of PAHs were also
152 extracted and used as blank soil samples. Analytes were quantified by using a gas
153 chromatograph (Hewlett-Packard G1099A/MSD5973) coupled to a mass spectrometer
154 (MSD5973). Separations were achieved on a DB-5 5% phenyl methyl siloxane column
155 (60 m x 0.25 mm x 0.25 µm). A volume of 1 µL of sample was injected at 310 ºC in
156 pulsed splitless mode, while the transfer line temperature was 280 ºC. The initial column
157 temperature was 90 ºC, being increased at a rate of 15 ºC min^{-1} up to 200 ºC, and then at
158 6 ºC min^{-1} until 325 ºC, being this temperature held for 20 min. Ultra-pure helium
159 (99.9999%) was the carrier gas at a flow rate of 1.4 mL min^{-1}. PAHs were quantified by

means of a five-point calibration curve (20, 30, 50, 70, 80 μg mL^{-1}). In order to allow the identification of PAHs degradation products as a second step of the experiment, the mass spectrometer was set at full scan mode instead of selected ion monitoring (SIM).

2.3. Quality control

To assess any potential loss, a mixture of 6 labeled PAHs (d_4-1,4-dichlorobenzene (99.8% purity), d_8-naphthalene (96.3% purity), d_{10}-acenaphthene (99.8% purity), d_{10}-phenanthrene (99.3% purity), d_{12}-chrysene (98.8% purity), and d_{12}-perylene (99.5% purity)), provided by Supelco® (Bellefonte, PA, USA), was spiked to soil samples before extraction. In turn, two individual deuterated PAHs, also from Supelco® (d_{10}-fluorene (98.3% purity) and d_{12}-benzo(*a*)pyrene (98.5% purity)), were added to samples before GC-MS analyses.

2.4. Identification of PAHs degradation products

Potential PAH by-products, generated as a consequence of soil exposure to solar radiation, were identified by using the MS library search NIST 11 (Scientific Instrument Services, Inc., Ringoes, NJ, USA). Afterwards, identified compounds were semi-quantified by considering peak areas. In addition, the correlations between their formation and the degradation of their parent compounds were graphically assessed. Therefore, possible degradation pathways occurring under sunlight exposure were also investigated.

2.5. Calculations

The equations to calculate photodegradation rates and half-lives of 16 PAHs were previously reported (Marquès et al., 2016a). In summary, these equations were the following:

$$L=\frac{C_N - C_I}{C_o} \times 100 \qquad \text{(Equation 1)}$$

where L is the photodegradation rate (in percentage) at time t, C_N is the concentration of the individual PAH in non-irradiated soil sample at time t, C_I is the concentration of the same PAH in irradiated sample at time t, and C_o is the initial PAH concentration.

$$ln\frac{C_o}{C_t} = k \cdot t \qquad \text{(Equation 2)}$$

193 $T_{1/2} = \frac{\ln 2}{k}$ (Equation 3)

194 where $T_{1/2}$ is the half-life of the individual PAH (in days), k is the apparent constant
195 reaction rate of the pseudo first order (1/day), t is the exposure time (in days), C_o is the
196 initial PAH concentration in soil (μg mL^{-1}), and C_t is the initial soil concentration of the
197 individual PAH (μg mL^{-1}).

198

199 **3. Results and discussion**

200

201 *3.1. PAH photodegradation rates and half-lives*

202

203 The average air temperature inside the box throughout the whole experiment was
204 14.4 ºC, with values ranging from 1.5 to 40.6 ºC. The mean global solar irradiance was
205 337.6 W m^{-2}, showing maximum irradiance peaks of 772 W m^{-2}. As expected, there was
206 some correlation between temperature and solar irradiance. Temperature *versus*
207 irradiance and environmental humidity *versus* precipitation are shown in Supplementary
208 Data (Fig. S1 and Fig. S2, respectively). The concentration of acenaphthylene,
209 anthracene, pyrene, benzo(*a*)pyrene and benzo(*ghi*)perylene, as representatives of
210 different molecular weight PAHs, in Arenosol and fine-textured Regosol soils exposed to
211 sunlight for 7 days, are depicted in Fig. 1. Details on the concentration changes of the
212 remaining PAHs are provided as Supplementary Information (Fig. S3). Photodegradation
213 rates and half-lives of the 16 PAHs are summarized in Table 1. The photodegradation rate
214 was estimated by considering only the impact of the sunlight exposure, as a difference
215 between irradiated and dark controls. In contrast, the half-life indicates the degradation
216 speed of a chemical exposed to solar radiation. It is due to sunlight exposure, but also due
217 to other co-occurring processes, such as volatilization, sorption or abiotic degradation.

218 The experiment was performed with dried soils. Consequently, the availability of
219 water was scarce. However, since the experiment was conducted in the field, it cannot be
220 disregarded that the increase of environmental humidity might have induced other
221 degradation processes, under the sunlight or in the darkness. Three main processes are
222 related to the fate of PAHs on surface soils: volatilization, sorption, and photodegradation
223 (Marquès et al., 2016a,b). Their importance depends not only on the physicochemical
224 properties of each hydrocarbon, but also on the soil texture. Volatilization was the most
225 important process for low molecular weight (LMW) PAHs, whose initial levels were low,

being the decrease of concentrations in dark controls more pronounced throughout the experiment. On the other hand, photodegradation was more remarkable for medium molecular weight (MMW) and HMW PAHs. Initial concentrations of the latter PAHs were higher, being the differences between irradiated and dark control samples more dependent on soil properties. LMW and MMW PAHs tended to undergo a higher photodegradation in fine-textured Regosol soil than in Arenosol soil. In contrast, HMW compounds (4-, 5-, and 6- ringed PAHs) were more easily photodegraded in Arenosol soil, with rates of up to 61 %. In general terms, most compounds presented lower half-lives in Arenosol soil, regardless their photodegradation rates.

Naphthalene and d_8-naphthalene were highly volatilized after soil was spiked with PAHs, being found very low concentrations, and without trends. Therefore, the results of naphthalene were not included and further investigated. The recoveries of the remaining PAHs ranged 54-106 % and 76 – 117 % in Arenosol and fine-textured Regosol soil, respectively.

The concentrations of acenaphthylene and acenaphthene dramatically decreased after soil contamination, as a consequence of the important role of volatilization for the loss of those PAHs. However, differences between irradiated and dark control samples indicated the impact of sunlight exposure, suggesting that photodegradation also occurred. In Arenosol soil, acenaphthylene and acenaphthene under solar radiation could not be detected shortly (24 and 72 h) after the experiment was started, leading to photodegradation rates of 50 % and 64 %, respectively (half-lives: 7.2 and 21.6 h, respectively). In turn, the decrease of these PAHs in fine-textured Regosol soil was softer, being quantified after 96 h of solar exposure. Since Regosol soils own a fine texture, they have an enhanced capacity to adsorb chemicals. The important differences of PAH loss between irradiated and dark control samples, led to high photodegradation rates (64.5 % and 54.6 % for acenaphthylene and acenaphthene, respectively), in comparison to Arenosol soil. It must be noted that the photodegradation of these 2 hydrocarbons was calculated taking into account the last detectable concentration, while for the rest of PAHs the final concentration considered was that at the end of the experiment (7th day). This could mean an overestimation of their photodegradation rates in front of those regarding other PAHs.

Fluorene, phenanthrene, anthracene and fluoranthene, all of them with 3 benzene rings, showed a similar behavior. However, there were some differences according to the soil texture. Their photodegradation rates were estimated in 61 %, 38 %, 54 % and 54 %,

respectively, in fine-textured soil samples. Moreover, they became the most highly photodegraded PAHs in this soil. In contrast, they were less photodegraded in Arenosol soil, with rates of 37 %, 29 %, 23 %, and 29 %, respectively. Although it is a heavier compound, benzo(*ghi*)perylene presented a similar behavior to those of MMW PAHs, being its photodegradation and half-life estimated in 21.5 % and 3.1 days, respectively. Lower half-lives were observed in Arenosol soil than in fine-textured Regosol soil, whose concentration trends were more pronounced. This difference would be due to the soil properties. Because of the coarse texture of the soil, the volatilization of 2- and 3- ringed PAHs is enhanced in Arenosol soil. In contrast, sorption plays a more relevant role in Regosol soil, which is characterized by a finer texture, and a higher organic matter content, making easier the penetration of sunlight exposure until deep layers. Finally, pyrene, benzo(*a*)anthracene, chrysene, dibenzo(*a,h*)anthracene and indeno(*123-cd*)perylene were highly photodegraded in Arenosol soil, with rates of 56 %, 50 %, 49 %, 39 % and 44 %, respectively. As isomer compounds, benzo(*b*)fluoranthene and benzo(*k*)fluoranthene presented similar half-lives in both soils (17.2 and 15.9 days, respectively), being also the most resistant PAHs to be photodegraded in Arenosol soil.

The remaining PAHs showed a similar degree of photodegradation in fine-textured Regosol soil, with a slight decrease of the photodegradation rate when the molecular weight increased. Pyrene and benzo(*a*)anthracene underwent photodegradations of 36 % and 34 %, respectively, being the half-lives estimated in 6.7 and 6.6 days, respectively. In addition to these 4-ringed PAHs, benzo(*b*)fluoranthene and benzo(*k*)fluoranthene presented photodegradation rates of 22 % and 26 %, respectively (half-lives: 8.4 and 9.2 days, respectively). Finally, the photodegradation of dibenzo(*a,h*)anthracene, indeno(*123-cd*)perylene and benzo(*ghi*)perylene ranged between 22 % and 27 %. In fine-textured Regosol soil, phenanthrene and chrysene were the most resistant to photodegradation, with half-lives of 13.0 and 11.2 days, respectively. Unlike Arenosol soil, fine-textured Regosol soil might have sorbed HMW PAHs more easily. Because of the small particle size of these soils, light cannot penetrate, reducing the photodegradation of LMW and MMW PAHs.

Anthracene showed short half-lives in both soils (1.9 and 2.6 days in Arenosol and fine-textured Regosol soils, respectively). In Arenosol soil, the concentration of this compound dramatically decreased over the time, not only in soils subjected to solar radiation, but also those in the darkness. In addition to volatilization, other degradation processes could be occurring in dark controls. On the other hand, in fine-textured Regosol

294 soil, anthracene did not probably experience changes in the darkness, leading therefore,
295 to a high photodegradation. In turn, benzo(*a*)pyrene underwent a very important
296 photodegradation in both soils, being that in Arenosol soil (61%) two-times higher than
297 that in fine-textured Regosol soil (30 %). Moreover, minor differences were noted in the
298 estimated half-lives (2.9 and 2.3 days, respectively). The levels of benzo(*a*)pyrene
299 remarkably decreased with time in all soils, both under solar radiation and in the darkness,
300 which was probably due to unknown degradation processes occurring without light
301 condition. Consequently, anthracene and benzo(*a*)pyrene were the most sensitive PAHs
302 to solar radiation in both tested soils.
303
304 *3.1.1. Comparing results: lab scale vs. field study*
305
306 The photodegradation of PAHs has been widely studied at laboratory scale by means
307 of natural or UV light lamps (Gupta and Gupta, 2015; Marquès et al., 2016a,b; Marquès
308 et al., 2016b; Zhang et al., 2006, 2008, 2010). Recently, we performed a similar
309 experiment with soils subjected to artificial light in a climate chamber (Marquès et al.,
310 2016a), considering various climate scenarios in terms of temperature (20ºC and 24ºC)
311 and light intensity (9.6 and 24 W/m^2). The results of the current study indicate that PAH
312 photodegradation is higher and quicker in the field than in lab-controlled tests, showing
313 all the chemicals a shorter half-life (Fig. 2). In the laboratory, LMW PAHs were only
314 volatilized. By contrast, in natural conditions, not only volatilization, but also
315 photodegradation could be detected as relevant degradation pathways. Half-lives of
316 MMW and HMW PAHs ranged between 3 and 80 days in soils exposed to artificial light
317 exposure. In turn, in the field experiment, they were remarkably lower, with half-life
318 values from 7 hours to 18 days.
319 Despite the photodegradation speed was more important in the field, concentration
320 trends of the individual PAHs were similar in both scenarios. Especially low half-lives of
321 anthracene and benzo(*a*)pyrene were found, resulting from their sensitivity to light
322 exposure and also other co-occurring degradation processes. Moreover,
323 benzo(*a*)anthracene, chrysene, benzo(*b*)fluoranthene and dibenzo(*a,h*)anthracene were
324 among the most resistant to photodegradation in both tested soils.
325 With respect to differences between soils, the higher content of iron, manganese and
326 aluminum oxides in fine-textured Regosol soil, was pointed out as a key factor when both
327 temperature and radiation are low, as these photocatalysts enhance photodegradation

328 reactions (Marquès et al., 2016b). In contrast, they had a very minor role when
329 temperature and light intensity were increased (Marquès et al., 2016a). As expected, a
330 similar pattern was found in the field experiment. Thus, the content of oxides in Regosol
331 soil did not lead to an enhancement of PAH photodegradation. As above-mentioned, the
332 coarse-texture of Arenosol soil facilitates a higher light penetration, leading to a higher
333 photodegradation.
334
335 *3.2. Identification of PAH photodegradation by-products*
336
337 The occurrence of PAH photodegradation by-products in irradiated samples was also
338 investigated. However, potential by-products resulting from other degradation processes,
339 such as biodegradation, generated either under radiation or in the darkness, were not here
340 considered. Up to 9 PAH degradation products were detected in the samples exposed to
341 sunlight for 7 days. The concentration trends, between the degradation of parent
342 compounds and the generation of by-products, are depicted in Figs. 3 and 4, respectively.
343 A number of aldehydes, oxy- PAHs, hydroxy-PAHs and nitro-PAHs were formed. Five
344 of them were already identified in our previous study performed at lab scale (Marquès et
345 al., 2016a). Nevertheless, they were more quickly generated under solar radiation.
346 Moreover, photodegradation reactions stepped forward by causing the formation of new
347 nitro- and hydroxy-PAHs.
348 Benzo(*a*)anthracene-7,12-dione, 1-acenaphthenol and 2-naphthalenecarboxaldehyde
349 were formed after 30 min of exposure to solar radiation in Arenosol and fine-textured
350 Regosol soil. It would be linked to the degradation of benzo(*a*)anthracene, acenaphthene
351 and naphthalene, respectively (Cajthaml et al., 2006; Marquès et al., 2016a; Woo et al.,
352 2009). There was a clear relationship between the formation of benzo(*a*)anthracene-7,12-
353 dione and the degradation of its precursor, benzo(*a*)anthracene, in both soils (Figs. 5a and
354 6a). In contrast, any relationship could not be found between the formation of 2-
355 naphthalenecarboxaldehyde and the degradation of naphthalene in Arenosol soil (Fig.
356 5b). It could be due to the high volatilization of the parent compound and/or the low
357 stability of this by-product. Although in fine-textured Regosol soil, 2-
358 naphthalenecarboxaldehyde was detected, a relative quantification could not be done.
359 A clear inverse correlation in the concentrations of 1-acenaphthenol and
360 acenaphthene was noted in fine-textured Regosol soil (Fig. 6b). Acenaphthene decreased,
361 while 1-acenaphthenol increased throughout the whole experiment. In Arenosol soil, 1-

acenaphthenol was firstly formed, and then its concentration started to decrease, probably due to soil dynamics (Fig. 5c). In this case, soil textures might be playing a key role. The coarse texture may enhance the light penetration, facilitating a quicker formation of 1-acenaphthenol in Arenosol soil. However, the texture and the low organic matter content of this soil do not allow the sorption of this by-product, favoring its volatilization and degradation.

Similarly, 1(2H)-acenaphthylenone, generated as a consequence of acenaphthylene oxidation (Woo et al., 2009), was more quickly formed under natural radiation. Again, generation processes depended on soil texture. 1(2H)-acenaphthylenone was found after half an hour of solar radiation in Arenosol soil, while it required 1 h of exposure in fine-textured Regosol soil. Correlations between the degradation of the acenaphthylene and the formation of the 1(2H)-acenaphthylenone were very clear (Fig. 5d and Fig. 6c). Naphthalic anhidridre was formed after half an hour and two hours of solar radiation exposure, in Arenosol and fine-textured Regosol soil, respectively. Potential precursors may be acenaphthylene and benzo(*a*)anthracene-7,12-dione (Cajthaml et al., 2006; Marquès et al., 2016a). Naphthalic anhidridre occurrence showed an increasing trend in Arenosol soil (Fig. 5e) and fine-textured Regosol soil (Fig. 5d). However, because naphthalene was not properly determined, no correlation with its parent compound could be detected. 9,10-phenanthrenedione, a PAH o-quinone photoproduct derived from phenanthrene (Kanaly and Hamamura, 2013), was fairly detected only in fine-textured Regosol soil for a short period of time (from 1 h to 3 h of solar light exposure).

At the end of the experiment, benzo(*a*)pyrene-7,8-dihydro was detected in Arenosol soil, being likely generated after the attachment of 2 hydroxyl radicals to benzo(*a*)pyrene. As the experiment lasted only 7 days, no more information could be retrieved regarding the fate of benzo(a)pyrene-7,8-dihydro in soils.

With respect to nitro-PAHs, 1-nitropyrene and 6-nitrobenzo(*a*)pyrene were detected in both soils. 1-nitropyrene was generated after only 2 h, while 6-nitrobenzo(*a*)pyrene was also formed, but at a slower rate (after 48 h of soil exposure). The formation of nitrated and oxygenated derivatives may occur through photo-reactions of PAHs with oxidative species such as ozone, hydroxyl and nitrate radicals, under UV radiation (Walgraeve et al., 2010; Zhang et al., 2011). In addition, the presence of NO_x radicals in soils can accelerate the formation of nitro-PAHs (Pham et al., 2015), by reacting with pyrene and benzo(*a*)pyrene. Sugiyama et al. (2001) demonstrated that nitrite (NO_2^-) and nitrate (NO_3^-) ions are sources of nitrated pyrenes in the presence of metallic oxides,

396 which act as photocatalysts. Both tested soils contained nitrates, aluminum, iron and
397 manganese oxides (Marquès et al., 2016b), which could have a key role on the formation
398 of nitro-PAHs. Nitro-PAHs generally exhibit higher mutagenicity and carcinogenicity
399 than their parent PAHs (Kameda, 2011), showing toxic effects for human health
400 (Nascimento et al., 2015). Some nitro-PAHs act directly as mutagens and carcinogens
401 on living organisms. In mammals, these chemicals may have a strong genotoxic
402 potential, being similar to or even higher than that of benzo(*a*)pyrene (Busby et al.,
403 1988; Onduka et al., 2015; Wislocki et al., 1986). 1-nitropyrene has been pointed out as
404 a mutagenic substance in many bacterial and mammalian assay systems, as well as
405 tumorigenic in experimentation animals (Hirose et al., 1984; McGregor et al., 1994;
406 Rosenkranz and and Mermelstein, 1983; Rosenkranz and Mermelstein, 1985; Watt et al.,
407 2007). In general terms, HMW nitro-PAHs tend to be resistant to photodegradation, partly
408 due to their strong adsorption to soil organic matter, low solubility, large molecular size
409 and polar character of the nitro group (Kielhorn et al., 2003). In addition, 6-
410 nitrobenzo(*a*)pyrene has been found as a potential NO donor due to its low stability,
411 inducing DNA strand breaks upon photoirradiation (Fukuhara et al., 2001).
412 Oxy-PAHs show a relatively high persistence, being usually formed in the practice of
413 remediation of PAH contaminated soils. Because of their polarity, oxy-PAHs are more
414 mobile in the environment than PAHs, showing a high tendency to spread from
415 contaminated sites via surface water and groundwater (Lundstedt et al., 2007).
416 Furthermore, they are also very bioavailable compounds (Arp et al., 2014).
417 Benzo(*a*)anthracene-7,12-dione induces similar or more elevated genotoxic responses
418 than their respective parent PAHs (Dasgupta et al., 2014; Gurbani et al., 2013). Its DNA
419 damage is in fact comparable to that produced by a well-known environmental mutagen,
420 benzo(*a*)pyrene, in fish embryos (Dasgupta et al., 2014).
421
422 **4. Conclusions**
423
424 Photodegradation is an important degradation pathway of PAHs in soil. Although this
425 subject has been largely studied in the past, most studies were performed at laboratory
426 scale. To the best of our knowledge, this is the first investigation aimed at assessing the
427 differences of PAH photodegradation in soils subjected to soil radiation and in lab-
428 controlled soil samples, exposed to light lamps. Our findings are very valuable to
429 determine the real impact of photodegradation in natural conditions, where other

430 degradation processes may be also occurring. The intensity of the solar radiation was
431 quantified to be 20-fold higher than that in the experiments conducted at laboratory scale.
432 This notable difference led to a higher photodegradation of PAHs in the field, being their
433 half-lives considerably shorter. LMW PAHs tended to leave quickly the soil through
434 volatilization. Photodegradation was more remarkable for LMW and MMW PAHs in
435 fine-textured Regosol soil, whereas this pathway played only a role for HMW PAHs in
436 Arenosol soil samples. Low half-lives were estimated for anthracene and benzo(*a*)pyrene,
437 while chrysene, benzo(*b*)fluoranthene and benzo(*k*)fluoranthene were the most resistant
438 PAHs to be photodegraded. Although similar trends were previously reported at a
439 laboratory scale (Marquès et al., 2016a), half-lives of PAHs in soils under solar radiation
440 were notably lower than values estimated in soils exposed to artificial light in a climate
441 chamber. It is a clear indication of the importance of photodegradation as a degradation
442 pathway of PAHs on surface soils in highly irradiated regions.

443 A number of photodegradation by-products were also generated after 7 days of soil
444 radiation, including a variety of aldehydes, oxy-, hydroxy- and nitro-PAHs. Although
445 some of them (e.g., 2-naphthalenecarboxaldehyde, naphthalic anhydride, 1-
446 acenaphthenol, 1(2H)-acenaphthylenone, and benzo(*a*)anthracene-7,12-dione) were
447 already identified at laboratory scale, their photodegradation was in the field. Moreover,
448 other nitro-PAHs (1-nitropyrene and 6-nitrobenzo(*a*)pyrene), hydroxy-PAHs
449 (benzo(*a*)pyrene-7,8-dihydro) and oxy-PAHs (9,10-phenanthrenedione) were also
450 detected throughout the experiment. Some of these photodegradation by-products, such
451 as 1-nitropyrene and 6-nitrobenzo(*a*)pyrene, exhibits a high mutagenic potential (Gurbani
452 et al., 2013).

453 Because of the lack of regulations and standardized methods for their analysis, oxy-
454 and nitro-PAHs are seldom included in monitoring and risk assessment programs
455 (Lundstedt et al., 2014). However, recent investigations on some of these by-products
456 have provided valuable information on their environmental occurrence and human
457 toxicity (Jörundsdóttir et al., 2014; Pinto et al., 2014; Qiao et al., 2014). Therefore,
458 environmental and health risks associated to exposure to these by-products is evident.
459 Since there is a gap on the environmental regulation of PAHs, it has been recently
460 suggested that that the original list of 16 US EPA priority PAHs should be enlarged by
461 including, at least, 10 oxy-PAHs, 10 nitro-PAHs and 6 amino-PAHs (Andersson and
462 Achten, 2015). Some of these PAH derivatives have been here identified as
463 photodegradation by-products. Anyhow, further investigations on their fate and behavior

should be conducted, paying especial attention to chemicals whose parent compounds are not only toxic, but also very photosensitive, like benzo(*a*)pyrene.

5. Acknowledgements

This study was supported by the Spanish Ministry of Economy and Competitiveness (Mineco), through the project CTM2012-33079. Montse Marquès received a PhD fellowship from AGAUR (Commissioner for Universities and Research of the Department of Innovation, Universities and Enterprise of the "Generalitat de Catalunya" and the European Social Fund). The authors are indebted to Dr. Irene Maijó for her excellent guidance and assistance in GC-MS analysis.

Appendix A. Supplementary data

Supplementary data associated with this article can be found, in the online version, at

6. References

Andersson J.T., Achten C., 2015. Time to say goodbye to the 16 EPA PAHs? Toward an up-to-date use of PACs for environmental purposes. Polycyclic Aromat. Compd. 35, 330-354.

Arp H.P.H., Lundstedt S., Josefsson S., Cornelissen G., Enell A., Allard A.-S., Kleja D.B., 2014. Native Oxy-PAHs, N-PACs, and PAHs in historically contaminated soils from Sweden, Belgium, and France: Their soil-porewater partitioning behavior, bioaccumulation in *Enchytraeus crypticus*, and bioavailability. Environ. Sci. Technol. 48, 11187−11195.

Augusto S., Sierra J., Nadal M., Schuhmacher M., 2015. Tracking polycyclic aromatic hydrocarbons in lichens: It's all about the algae. Environ. Pollut. 2015, 441-445.

Batchu S.R., Panditi V.R., O'Shea K.E., Gardinali P.R., 2014. Photodegradation of antibiotics under simulated solar radiation: Implications for their environmental fate. Sci. Total Environ. 470-471, 299-310.

Borrás E., Ródenas M., Vázquez M., Vera T., Muñoz A., 2015. Particulate and gas-phase products from the atmospheric degradation of chlorpyrifos and chlorpyrifos-oxon. Atmos. Environ. 123, 112-120.

Busby W.J., Stevens E., Kellenbach E., Cornelisse J., Lugtenburg J., 1988. Dose-response relationships of the tumorigenicity of cyclopenta(*cd*)pyrene, benzo(*a*)pyrene and 6-nitrochrysene in a newborn mouse lung adenoma bioassay. Carcinogenesis 9, 741-746.

Cajthaml T., Erbanová P., Šašek V., Moeder M., 2006. Breakdown products on metabolic pathway of degradation of benz(*a*)anthracene by a ligninolytic fungus. Chemosphere 64, 560-564.

Chen F., Tan M., Ma J., Zhang S., Li G., Qu J., 2016. Efficient remediation of PAH-metal co-contaminated soil using microbial-plant combination: A greenhouse study. J. Hazard. Mater. 302, 250-261.

Dasgupta S., Cao A., Mauer B., Yan B., Uno S., McElroy A., 2014. Genotoxicity of oxy-PAHs to Japanese medaka (*Oryzias latipes*) embryos assessed using the comet assay. Environ. Sci. Pollut. Res. 21, 13867-13876.

Domingo J.L., Nadal M., 2015. Human dietary exposure to polycyclic aromatic hydrocarbons: A review of the scientific literature. Food Chem. Toxicol. 86, 144-153.

EL-Saeid M.H., Al-Turki A.M., Nadeem M.E.A., Hassanin A.S., Al-Wabel M.I., 2015. Photolysis degradation of polyaromatic hydrocarbons (PAHs) on surface sandy soil. Environ. Sci. Pollut. Res. 22, 9603–9616.

Fu P.P., Xia Q., Sun X., Yu H., 2012. Phototoxicity and environmental transformation of polycyclic aromatic hydrocarbons (PAHs)-light-induced reactive oxygen species, lipid peroxidation, and DNA damage. J. Environ. Sci. Health Part C Environ. Carcinog. Ecotoxicol. Rev. 30, 1-41.

Fukuhara K., Kurihara M., Miyata N., 2001. Photochemical generation of nitric oxide from 6-nitrobenzo(a)pyrene. J. Am. Chem. Soc. 123, 8662–8666.

Ge L., Chen J., Wei X., Zhang S., Qiao X., Cai X., Xie Q., 2010. Aquatic photochemistry of fluoroquinolone antibiotics: kinetics, pathways, and multivariate effects of main water constituents. Environ. Sci. Technol. 44.

Gupta H., Gupta B., 2015. Photocatalytic degradation of polycyclic aromatic hydrocarbon benzo[a]pyrene by iron oxides and identification of degradation products. Chemosphere.

Gurbani D., Bharti S.K., Kumar A., Pandey A.K., Ana G.R.E.E., Verma A., Khan A.H., Patel D.K., Mudiam M.K.R., Jain S.K., Raja Royf A.D., 2013. Polycyclic aromatic hydrocarbons and their quinones modulate the metabolic profile and induce DNA damage in human alveolar and bronchiolar cells. Int. J. Hyg. Environ. Health 216, 553-565.

Hirose M., Lee M.S., Wang C.Y., King C.M., 1984. Induction of rat mammary gland tumors by 1-nitropyrene, a recently recognized environmental mutagen. Cancer Res. 44, 1158-1162.

Hu N.-J., Huang P., Liu J.-H., Ma D., Shi X.-F., Mao J., Liu Y., 2014. Characterization and source apportionment of polycyclic aromatic hydrocarbons (PAHs) in sediments in the Yellow River Estuary, China. Environ. Earth Sci. 71, 873-883.

Hung H., Blanchard P., Halsall C.J., Bidleman T.F., Stern G.A., Fellin P., Muir D.C.G., Barrie L.A., Jantunen L.M., Helm P.A., Ma J., Konoplev A., 2005. Temporal and spatial variabilities of atmospheric polychlorinated biphenyls (PCBs), organochlorine (OC) pesticides and polycyclic aromatic hydrocarbons (PAHs) in the Canadian Arctic: Results from a decade of monitoring. Sci. Total Environ. 342, 119-144.

Jia H., Li L., Chen H., Zhao Y., Li X., Wang C., 2015. Exchangeable cations-mediated photodegradation of polycyclic aromatic hydrocarbons (PAHs) on smectite surface under visible light. J. Hazard. Mater. 287, 16-23.

Jörundsdóttir H.Ó., Jensen S., Hylland K., Holth T.F., Gunnlaugsdóttir H., Svavarsson J., Ólafsdóttir Á., El-Taliawy H., Rigét F., Strand J., Nyberg E., Bignert A., Hoydal K.S., Halldórsson H.P., 2014. Pristine Arctic: Background mapping of PAHs, PAH metabolites and inorganic trace elements in the North-Atlantic Arctic and sub-Arctic coastal environment. Sci. Total Environ. 493, 719-728.

Kameda T., 2011. Atmospheric Chemistry of Polycyclic Aromatic Hydrocarbons and Related Compounds. J. Health Sci. 57, 504-511.

Kanaly R.A., Hamamura N., 2013. 9,10-Phenanthrenedione biodegradation by a soil bacterium and identification of transformation products by LC/ESI-MS/MS. Chemosphere 92, 1442-1449.

Kielhorn J., Wahnschaffe U., Mangelsdorf I. Environmental Health Criteria 229: Selected nitro- and nitro-oxy-polycyclic aromatic hydrocarbons. Environ. Health Criter. 229, 2003, pp. i-480.

Lundstedt S., Bandowe B.A.M., Wilcke W., Boll E., Christensen J.H., Vila J., Grifoll M., Faure P., Biache C., Lorgeoux C., Larsson M., Irgum K.F., Ivarsson P., Ricci M., 2014. First intercomparison study on the analysis of oxygenated polycyclic aromatic hydrocarbons (oxy-PAHs) and nitrogen heterocyclic polycyclic aromatic compounds (N-PACs) in contaminated soil. Trends Anal. Chem. 57, 83-92.

Lundstedt S., White P.A., Lemieux C.L., Lynes K.D., Lambert I.B., Öberg L., Haglund P., Tysklind M., 2007. Sources, Fate, and Toxic Hazards of Oxygenated Polycyclic Aromatic Hydrocarbons (PAHs) at PAH-Contaminated Sites. Ambio 36.

Marquès M., Mari M., Audí-Miró C., Sierra J., Soler A., Nadal M., Domingo J.L., 2016a. Climate change impact on the PAH photodegradation in soils: Characterization and metabolites identification. Environ. Int. 89-90, 155-165.

Marquès M., Mari M., Audí-Miró C., Sierra J., Soler A., Nadal M., Domingo J.L., 2016b. Photodegradation of polycyclic aromatic hydrocarbons in soils under a climate change base scenario. Chemosphere 148, 495-503.

McGregor W.G., Maher V.M., McCormick J.J., 1994. Kinds and locations of mutations induced in the hypoxanthine-guanine phosphoribosyltransferase gene of human T-lymphocytes by 1-nitrosopyrene, including those caused by V(D)J recombinase. Cancer Res. 54, 4207-4213.

Muñoz A., Vera T., Ródenas M., Borrás E., Mellouki A., Treacy J., Sidebottom H., 2014. Gas-phase degradation of the herbicide ethalfluralin under atmospheric conditions. Chemosphere 95, 395-401.

Nadal M., Mari M., Schuhmacher M., Domingo J.L., 2009. Multi-compartmental environmental surveillance of a petrochemical area: Levels of micropollutants. Environ. Int. 35, 227-235.

Nadal M., Schuhmacher M., Domingo J.L., 2011. Long-term environmental monitoring of persistent organic pollutants and metals in a chemical/petrochemical area: Human health risks. Environ. Pollut. 159, 1769-1777.

Nascimento P.C., Gobo L.A., Bohrer D., Carvalho L.M., Cravo M.C., Leite L.F.M., 2015. Determination of oxygen and nitrogen derivatives of polycyclic aromatic hydrocarbons in fractions of asphalt mixtures using liquid chromatography coupled to mass spectrometry with atmospheric pressure chemical ionization. J. Sep. Sci. 38, 4055-4062.

Ohkouchi N., Kawamura K., Kawahata H., 1999. Distribution of threeto seven-ring polycyclic aromatic hydrocarbons on the deep sea floor in the central Pacific. Environ. Sci. Technol. 33, 3086-3090.

Onduka T., Ojima D., Mochida K.I., Koyama J., Fujii K., 2015. Reproductive toxicity of 1-nitronaphthalene and 1-nitropyrene exposure in the mummichog, Fundulus heteroclitus. Ecotoxicology 24, 648-656.

Pereira K.L., Hamilton J.F., Rickard A.R., Bloss W.J., Alam M.S., Camredon M., Ward M.W., Wyche K.P., Muñoz A., Vera T., Vázquez M., Borrás E., Ródenas M., 2015. Insights into the Formation and Evolution of Individual Compounds in the Particulate Phase during Aromatic Photo-Oxidation. Environ. Sci. Technol. 49, 13168-13178.

Pereira V.J., Weinberg H.S., Linden K.G., Singer P.C., 2007. UV degradation kinetics and modeling of pharmaceutical compounds in laboratory grade and surface Water via direct and indirect photolysis at 254 nm. Environ. Sci. Technol. 41, 1682-1688.

Pham C.T., Tang N., Toriba A., Hayakawa K., 2015. Polycyclic Aromatic Hydrocarbons and Nitropolycyclic Aromatic Hydrocarbons in atmospheric particles and soil at a traffic site in Hanoi, Vietnam. Polycyclic Aromat. Compd. 35, 355-371.

Pinto M., Costa P.M., Louro H., Costa M.H., Lavinha J., Caeiro S., Silva M.J., 2014. Determining oxidative and non-oxidative genotoxic effects driven by estuarine sediment contaminants on a human hepatoma cell line. Sci. Total Environ. 478, 25-35.

Qiao M., Qi W., Liu H., Qu J., 2014. Oxygenated, nitrated, methyl and parent polycyclic aromatic hydrocarbons in rivers of Haihe River System, China: Occurrence, possible formation, and source and fate in a water-shortage area. Sci. Total Environ. 481, 178-185.

Ras M.R., Marcé R.M., Cuadras A., Mari M., Nadal M., Borrull F., 2009. Atmospheric levels of polycyclic aromatic hydrocarbons in gas and particulate phases from Tarragona Region (NE Spain). Int. J. Environ. Anal. Chem. 89, 543-556.

Rosenkranz H.S., and Mermelstein R., 1983. Mutagenicity and genotoxicity of nitroarenes. All nitro-containing chemicals were not created equal. Mutat. Res/Rev. Genet. 114, 217-267.

Rosenkranz H.S., Mermelstein R., 1985. The genotoxicity, metabolism, and carcinogenicity of nitrated polycyclic aromatic hydrocarbons. J. Environ. Sci. Health Part C Environ. Carcinog. Rev. 3, 221-272.

Sugiyama H., Watanabe T., Hirayama T., 2001. Nitration of pyrene in metallic oxides as soil components in the presence of indoor air, nitrogen dioxide gas, nitrite ion, or nitrate ion under xenon irradiation. J. Health Sci. 47, 28-35.

Vera T., Borrás E., Chen J., Coscollá C., Daële V., Mellouki A., Ródenas M., Sidebottom H., Sun X., Yusá V., Zhang X., Muñoz A., 2015. Atmospheric degradation of lindane and 1,3-dichloroacetone in the gas phase. Studies at the EUPHORE simulation chamber. Chemosphere 138, 112-119.

Walgraeve C., Demeestere K., Dewulf J., Zimmermann R., Langenhove H.V., 2010. Oxygenated polycyclic aromatic hydrocarbons in atmospheric particulate matter: Molecular characterization and occurrence. Atmos. Environ. 44, 1831-1846.

Watt D.L., Utzat C.D., Hilario P., Basu A.K., 2007. Mutagenicity of the 1-Nitropyrene-DNA Adduct N-(Deoxyguanosin-8-yl)-1-aminopyrene in Mammalian Cells. Chem. Res. Toxicol. 20, 1658-1664.

Wislocki P.G., Bagan E.S., Lu A.Y.H., Dooley K.L., Fu P.P., Han-Hsu H., Beland F.A., Kadlubar F.F., 1986. Tumorigenicity of nitrated derivatives of pyrene, benzo(*a*)anthracene, chrysene and benzo(*a*)pyrene in the newborn mouse assay. Carcinogenesis 7, 1317-1322.

Woo O.T., Chung W.K., Wong K.H., Chow A.T., P.K.Wong. 2009. Photocatalytic oxidation of polycyclic aromatic hydrocarbons: Intermediates identification and toxicity testing. J. Hazard. Mater. 168, 1192-1199.

Zhang L., Li P., Gong Z., Oni A., 2006. Photochemical behavior of benzo[*a*]pyrene on soil surfaces under UV light irradiation. J. Environ. Sci. 18, 1226-1232.

Zhang L., Li P., Gong Z., Li X., 2008. Photocatalytic degradation of polycyclic aromatic hydrocarbons on soil surfaces using TiO_2 under UV light. J. Hazard. Mater. 158, 478-484.

Zhang L., Xua C., Chena Z., Li X., Li P., 2010. Photodegradation of pyrene on soil surfaces under UV light irradiation. J. Hazard. Mater. 173, 168-172.

Zhang Y., Yang B., Gan J., Liu C., Shu X., Shu J., 2011. Nitration of particle-associated PAHs and their derivatives (nitro-, oxy-, and hydroxy-PAHs) with NO_3 radicals. Atmos. Environ. 45, 2515-2521.

641

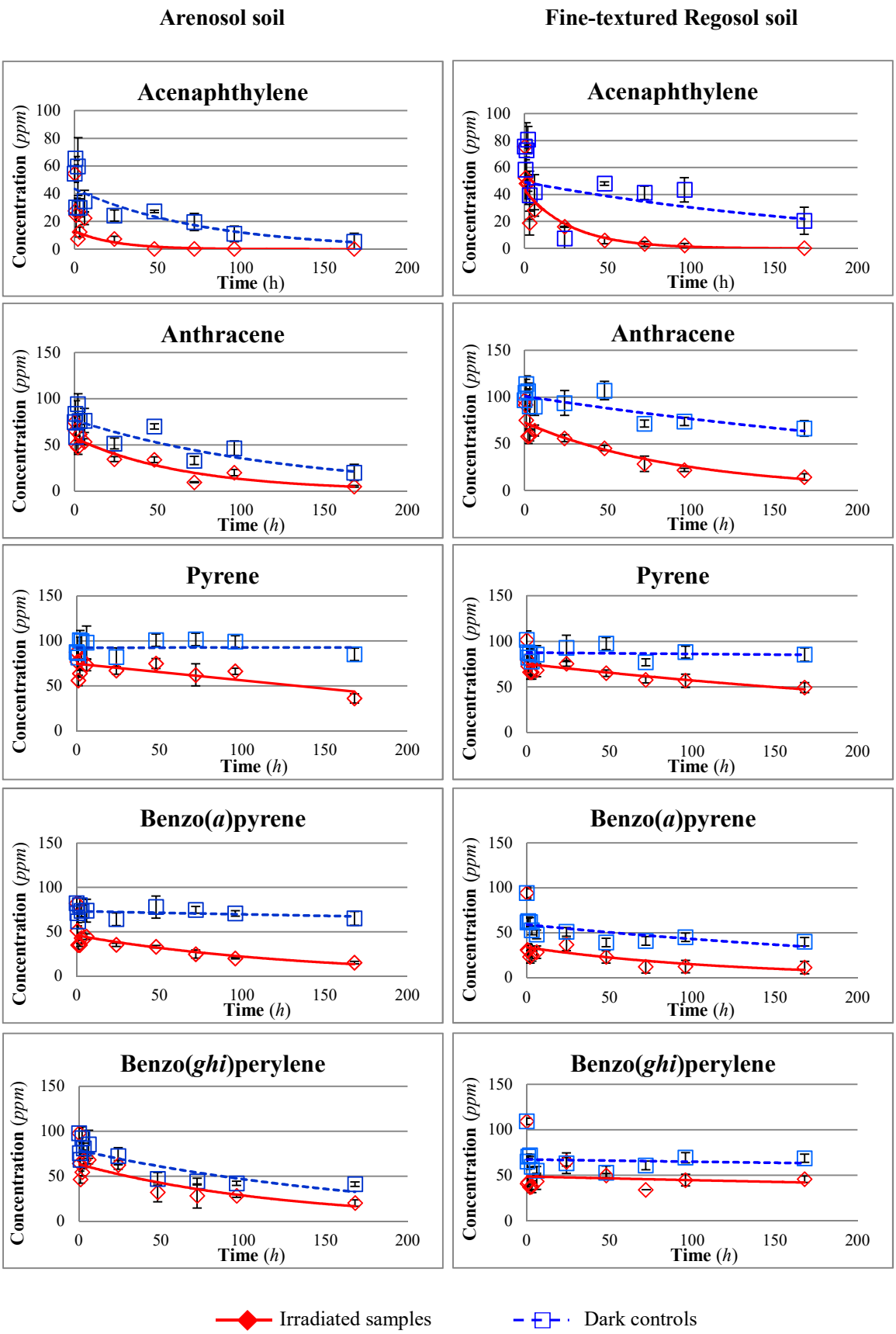

Fig. 1. Concentration trends of acenaphthylene, anthracene, pyrene, benzo(*a*)pyrene and benzo(*ghi*)perylene in Arenosol soil (left) and fine-textured Regosol soil (right). Bars indicate standard deviations between triplicates of samples.

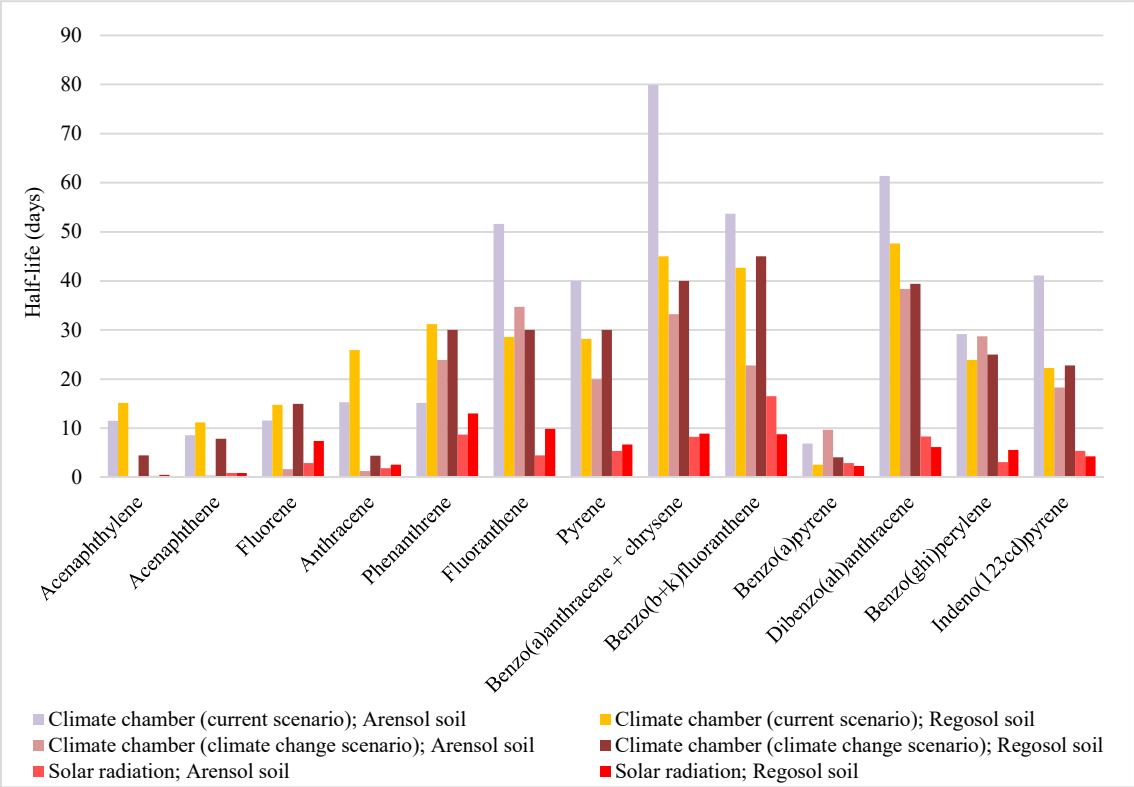

Fig. 2. Comparison between half-lives of PAHs when simulating different climate scenarios at lab scale (adapted from Marquès et al., 2016a], and the current experiment in the field, for both tested soils.

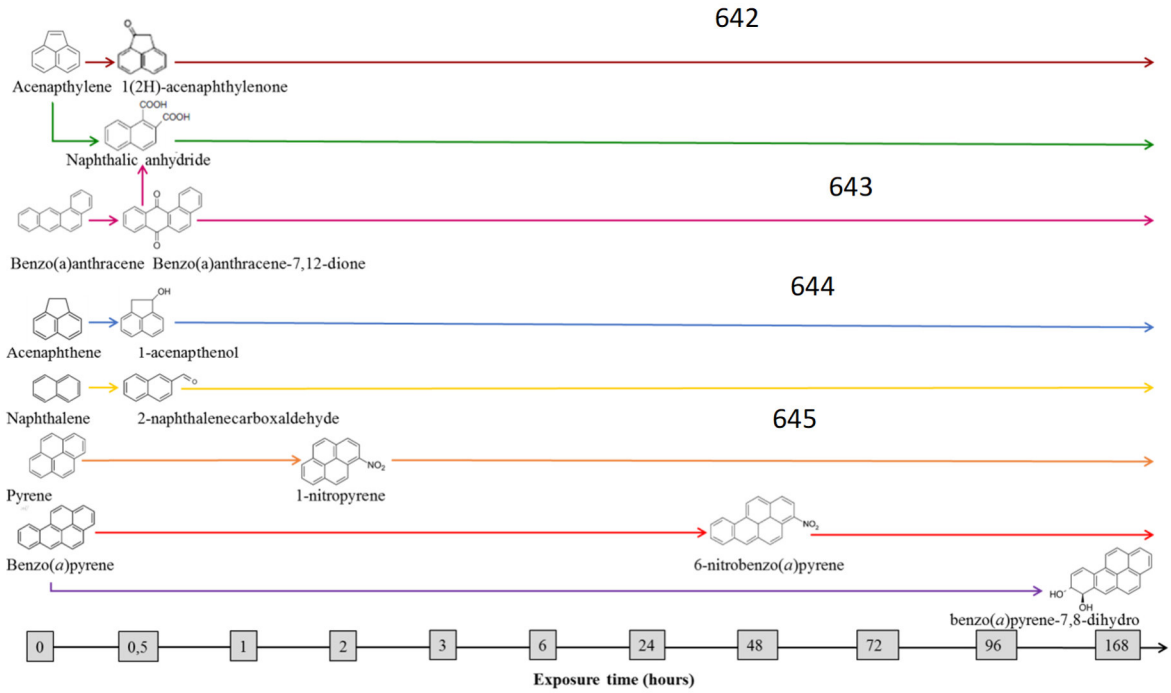

Fig. 3. Potential degradation pathways due to degradation of PAHs in samples of Arenosol soil exposed to solar radiation.

646

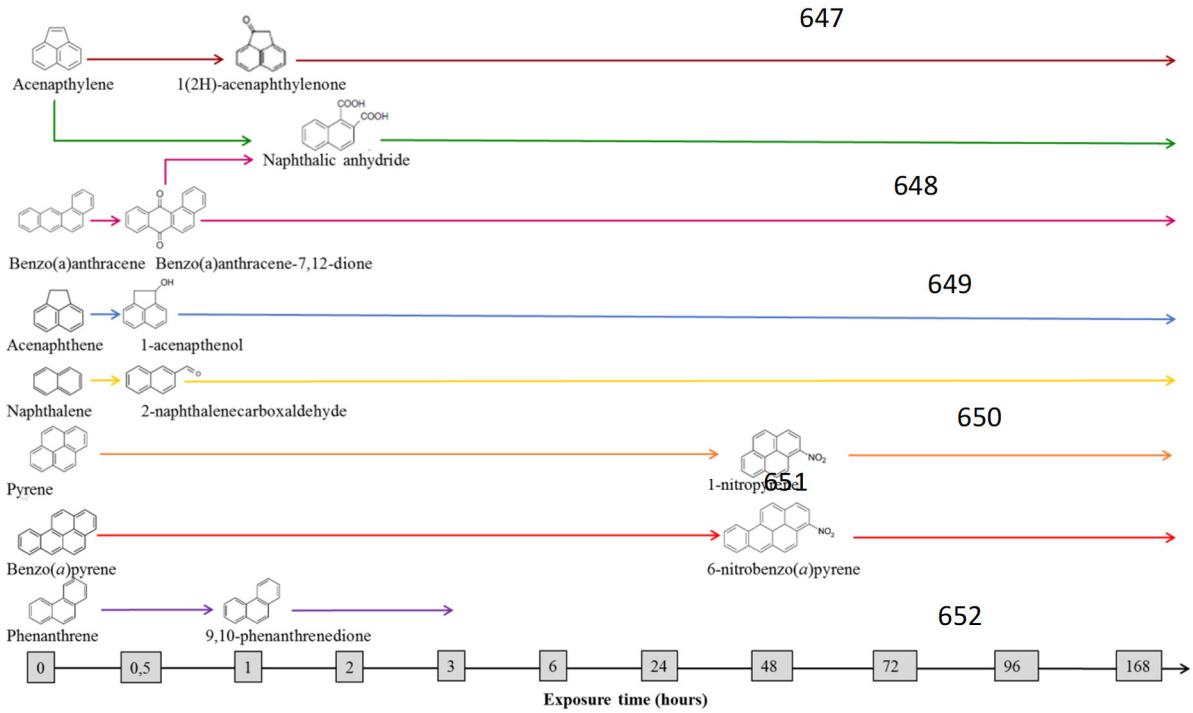

Fig. 4. Potential degradation pathways due to degradation of PAHs in samples of fine-textured Regosol soil exposed to solar radiation.

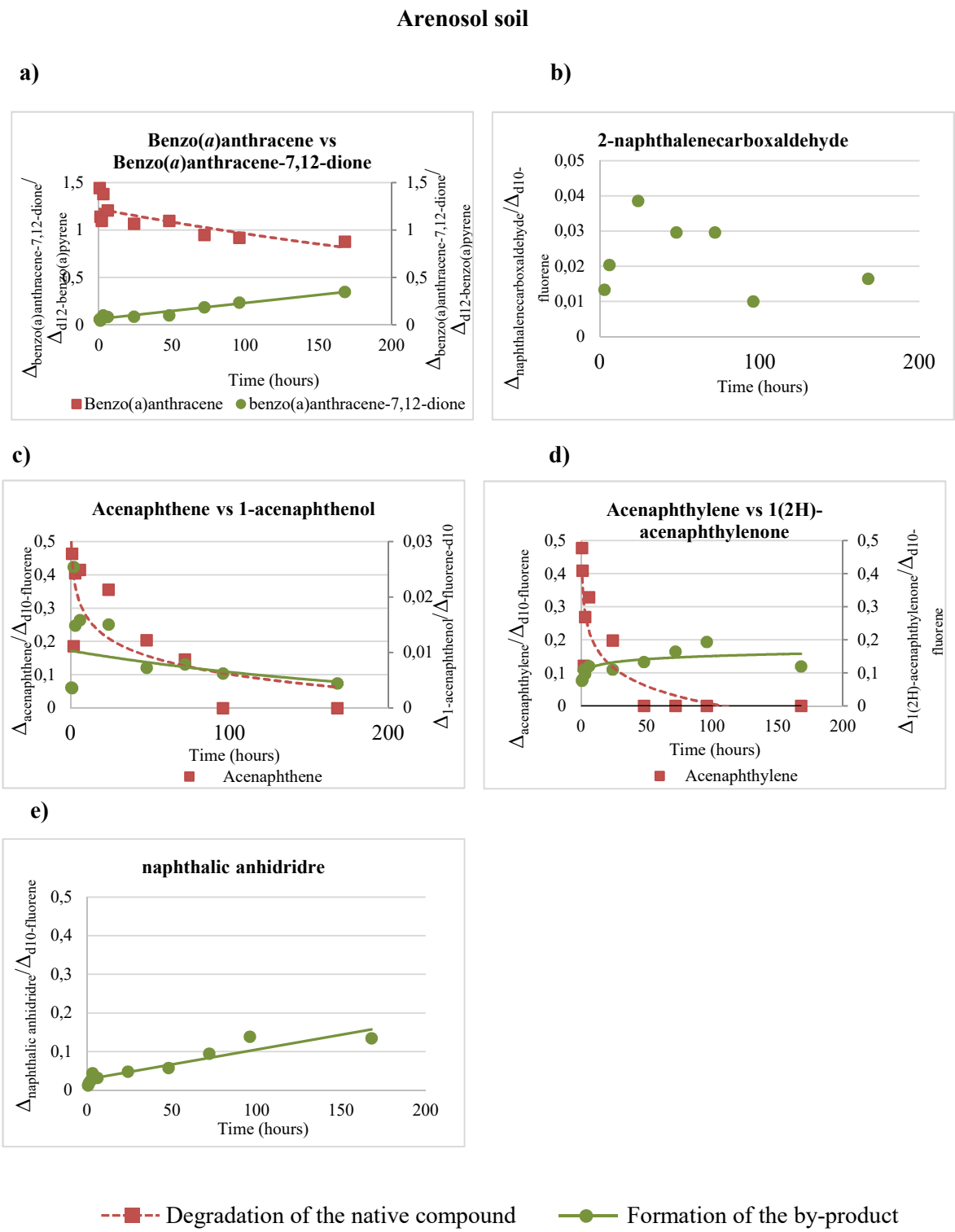

Fig. 5. Native PAHs degradation vs corresponding PAH by-products formation.

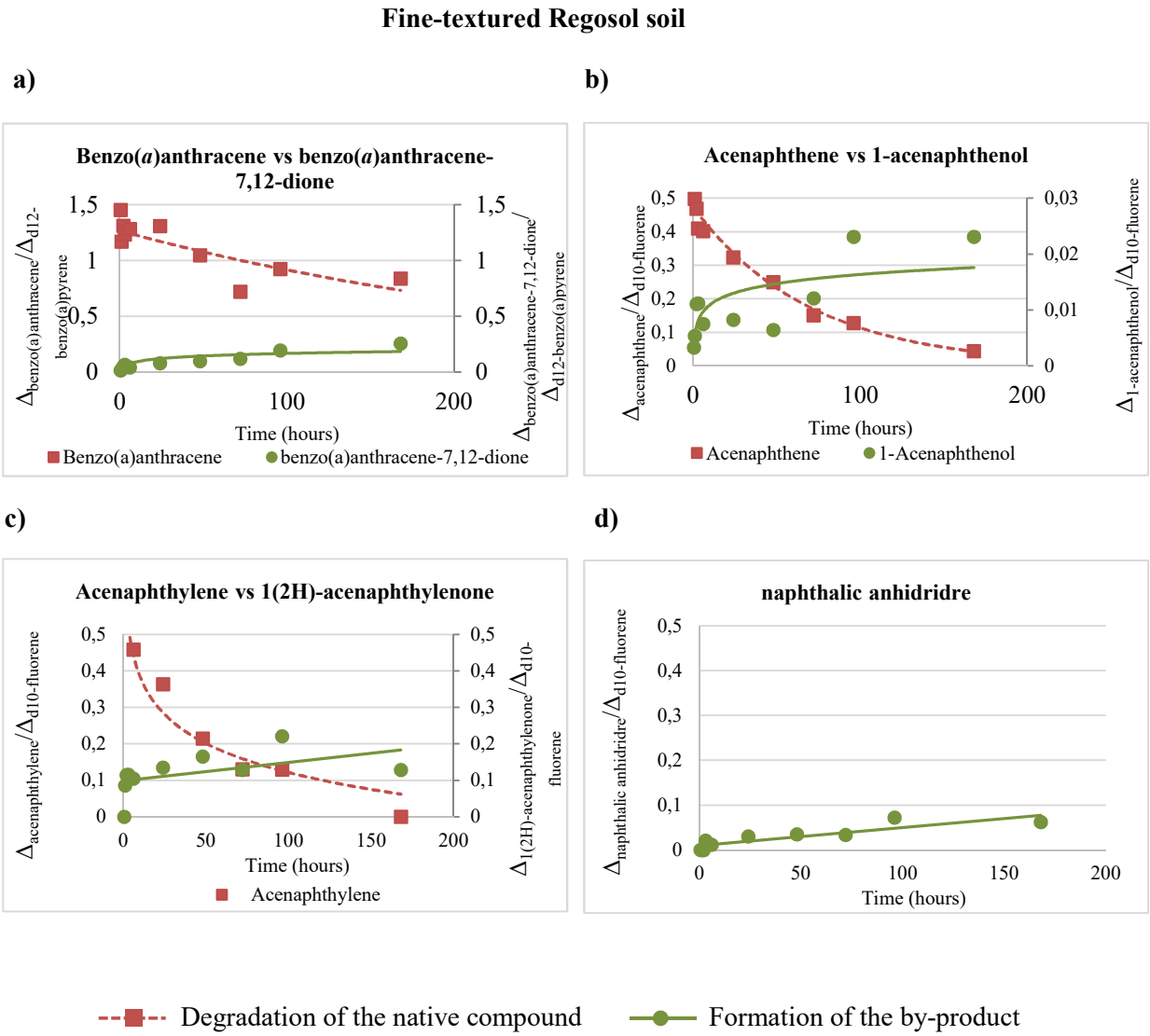

Fig. 6. Selected native PAHs degradation vs corresponding PAH by-products formation.

Table 1

Photodegradation rates and half-lives of PAHs under study in Arenosol and fine-textured Regosol soil

	Arenosol soil		Fine-textured Regosol soil	
	Photodegradation rate (%)	Half-live (days)	Photodegradation rate (%)	Half-live (days)
Acenaphthylene	50.0[a]	0.3[a]	64.5[c]	0.5[c]
Acenaphthene	63.6[b]	0.9[b]	54.6[c]	0.9[c]
Fluorene	36.6	2.9	61.0	7.4
Phenanthrene	28.6	8.7	38.0	13.0
Anthracene	23.0	1.9	53.6	2.6
Fluoranthene	28.5	4.5	53.7	9.9
Pyrene	56.0	5.4	35.6	6.7
Benzo(*a*)anthracene	50.3	7.8	33.7	6.6
Chrysene	48.9	8.7	13.5	11.2
Benzo(*b*)fluoranthene	25.5	17.2	22.4	8.4
Benzo(*k*)fluoranthene	14.8	15.9	26.4	9.2
Benzo(*a*)pyrene	61.0	2.9	30.4	2.3
Benzo(*ghi*)perylene	21.5	3.1	23.0	6.2
Dibenzo(*a,h*)anthracene	38.6	8.3	21.7	5.6
Indeno(*123-cd*)perylene	44.0	5.4	26.8	4.3

[a,b,c] Complete disappearance after [a]24 hours, [b]72 h or [c]96 h of solar radiation exposure